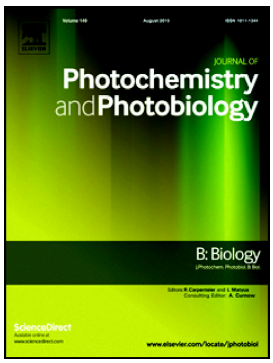

In vitro photodynamic activity of lipid vesicles with zinc phthalocyanine derivative against Enterococcus faecalis

Lukasz Sobotta, Jolanta Dlugaszewska, Piotr Kasprzycki, Sebastian Lijewski, Anna Teubert, Jadwiga Mielcarek, Maria Gdaniec, Tomasz Goslinski, Piotr Fita, Ewa Tykarska

PII: S1011-1344(18)30235-5
DOI: doi:10.1016/j.jphotobiol.2018.04.025
Reference: JPB 11208

To appear in: *Journal of Photochemistry & Photobiology, B: Biology*

Received date: 28 February 2018
Revised date: 10 April 2018
Accepted date: 14 April 2018

Please cite this article as: Lukasz Sobotta, Jolanta Dlugaszewska, Piotr Kasprzycki, Sebastian Lijewski, Anna Teubert, Jadwiga Mielcarek, Maria Gdaniec, Tomasz Goslinski, Piotr Fita, Ewa Tykarska , In vitro photodynamic activity of lipid vesicles with zinc phthalocyanine derivative against Enterococcus faecalis. The address for the corresponding author was captured as affiliation for all authors. Please check if appropriate. Jpb(2018), doi:10.1016/j.jphotobiol.2018.04.025

In vitro photodynamic activity of lipid vesicles with zinc phthalocyanine derivative against *Enterococcus faecalis*

Lukasz Sobotta[a,*], Jolanta Dlugaszewska[b], Piotr Kasprzycki[c], Sebastian Lijewski[d], Anna Teubert[e], Jadwiga Mielcarek[a], Maria Gdaniec[f], Tomasz Goslinski[d], Piotr Fita[c], Ewa Tykarska[d]

[a]*Department of Inorganic and Analytical Chemistry, Poznan University of Medical Sciences, Grunwaldzka 6, 60-780 Poznan, Poland*

[b]*Department of Genetics and Pharmaceutical Microbiology, Poznan University of Medical Sciences, Swiecickiego 4, 60-780 Poznan, Poland*

[c]*Institute of Experimental Physics, Faculty of Physics, University of Warsaw, Pasteura 5, 02-093 Warsaw, Poland*

[d]*Department of Chemical Technology of Drugs, Poznan University of Medical Sciences, Grunwaldzka 6, 60-780 Poznan, Poland*

[e]*Institute of Bioorganic Chemistry, Polish Academy of Sciences, Z. Noskowskiego 12/14, Poznan, Poland*

[f]*Faculty of Chemistry, Adam Mickiewicz University, Umultowska 89b, 61-614 Poznan, Poland*

ABSTRACT

Zinc(II) phthalocyanine bearing eight non-peripheral 2-propoxy substituents was subjected to physicochemical study and, after incorporation in lipid vesicles, assessed as a potential photosensitizer for antibacterial photodynamic therapy. The phthalocyanine derivative obtained in the macrocyclization reaction was characterized by MS and NMR techniques. Moreover, its chemical purity was confirmed by HPLC analysis. X-ray structural analysis revealed that overcrowding of the phthalocyanine derivative leads to a strong out-of-plane distortion of the π-system of the macrocycle core. In the UV-Vis absorption spectra of zinc(II) phthalocyanine two characteristic bands were found: the Soret (300–450 nm) and the Q band (600–800 nm). Photophysical properties of mono- and diprotonated forms of phthalocyanine derivative were studied with time-resolved fluorescence spectroscopy. Its tri- and tetraprotonated forms could not be obtained, because compound decomposing in higher acid concentrations. The presented zinc(II) phthalocyanine showed values of singlet oxygen generation Φ_{Δ} = 0.18 and 0.16, the quantum yield of the photodecomposition $\Phi_{P} = 3.06 \cdot 10^{-4}$ and $1.23 \cdot 10^{-5}$ and the quantum yield of fluorescence Φ_{FL} = 0.005 and 0.004, designated in DMF and DMSO, respectively. For biological studies, phthalocyanine has been incorporated into modified liposome vesicles containing ethanol. *In vitro* bacteria photoinactivation study revealed no activity against *Escherichia coli* and 5.7 log reduction of the *Enterococcus faecalis* growth.

KEYWORDS: phthalocyanines, singlet oxygen, X-ray, PACT, *Enterococcus faecalis*

*Corresponding author

E-mail address: lsobotta@ump.edu.pl (L. Sobotta).

1. Introduction

Phthalocyanines (Pcs) belong to a group of aromatic macroheterocycles and consist of four isoindole units linked together with azamethine bridges. Due to their complex structure Pcs exhibit unique spectro-, photo- and electrochemical properties. Therefore, they can be applied in many fields of technology and industry, i.e. as dyes, in photovoltaics, in medicine, etc. [1–6]. Pcs excited with visible light in a photodynamic process can generate singlet oxygen and other equally reactive oxygen species. Especially, highly energetic singlet oxygen can react in living organisms with biologically active substrates disturbing its functions and finally leading to apoptotic and/or necrotic cell death [7]. This phenomenon enables the application of Pcs in medicine as photosensitizers (PS) for photodynamic therapy (PDT) [8,9]. PDT is a treatment method of cancer lesions, psoriasis, actinic keratosis, in dermatology for photorejuvenation and many others. PDT possesses some advantages in comparison to conventional treatment methods, especially chemotherapy and radiotherapy. Moreover, antimicrobial PDT reveals potential applications *in vitro* and *in vivo* study against viral and bacterial infections [10–13]. The challenge would be to develop novel antibiotics and antimicrobial therapies. The amount of reports on the bacterial resistance to antibiotics is rising. For this reason, current scientific research concerns methods of treatment in the upcoming post-antibiotic era [11]. Photodynamic Antimicrobial Chemotherapy (PACT) is a medical approach worth developing, as it can provide interesting alternatives and solutions to diminish growing bacterial resistance. The potential clinical use of this procedure has been so far limited mainly to the treatment of local skin or mucosa infections, but the amount of other clinical studies has been rapidly growing, among others for the treatment of malaria and trypanosomiasis [14–17]. Recently, photosensitizers synthesized and researched for modern PACT in many *in vitro* and *in vivo* studies revealed the potential of a synergistic effect in combination with antibiotics [18].

Photosensitizers often possess a highly hydrophobic nature, which complicates drug administration. This limitation can be overcome by modifying macrocycle molecules or applying pharmaceutical formulations, for instance, liposomes or cyclodextrins [19,20]. Our group has developed many porphyrazine and phthalocyanine photosensitizers and evaluated their biological activity *in vitro* against various cancer cells [21–23], bacteria [24] and viruses [22]. Lately, for the delivery of photosensitizers, various vesicular systems embodying ethanol, have been proposed, including modified liposome vesicles known as invasomes and ethosomes. Invasomes besides common phospholipid ingredients and ethanol contain

terpenes. The optimal concentration of ethanol makes the lipid vesicle membrane more flexible and increases the delivery of biologically active ingredients into the skin or enhances its penetration through the biological membranes [25]. The flexibility of invasomes is a desirable property. These carriers containing photosensitizer mTHPC were proposed for the inactivation of *Enterococcus faecalis*, which is the leading pathogen causing periapical changes in teeth as it penetrates into dentinal tubules. Dentinal tubules diameters are in the range of 0.9 up to 2.5 μm, which enable bacteria to go inside the tubules and persist the treatment. It has been proved that invasomes can be considered as a useful carrier for the delivery of photosensitizer [26]. In this study, we have focused on photodynamic inactivation of bacteria with novel zinc(II) phthalocyanine derivative. Therefore, we have synthesized a zinc phthalocyanine derivative and assessed its photophysical and photochemical properties. After that, the *in vitro* antibacterial PACT potential of this photosensitizer incorporated in lipid vesicular systems embodying the optimal concentration of ethanol was evaluated.

2. Experimental

2.1. General

All reactions were carried out in oven-dried glassware under inert gas atmosphere. Reaction temperature refers to external bath temperature. Solvents were distilled before use. Other solvents and all reagents were obtained from commercial suppliers and used without further purification. Flash column chromatography was carried out on Merck silica gel 60, particle size 40-63 μm. Reversed-phase column chromatography was performed on Fluka Silica gel C_{18}. Thin layer chromatography (TLC) was performed on silica gel Merck Kieselgel 60 F_{254} plates and visualized with UV (λ_{max} 254 or 365 nm). UV-Vis spectra were recorded on a Hitachi UV-Vis U-1900 spectrophotometer: λ_{max} [nm] (log ε). ^{1}H NMR, ^{13}C NMR spectra were recorded using a Bruker 400 spectrometer. Chemical shifts (δ) are quoted in parts per million (ppm) and are referred to a residual solvent peak. Coupling constants (J) are quoted in Hertz (Hz) to the nearest 0.5 Hz. The abbreviations s, d and m refer to singlet, doublet, and multiplet, respectively. MALDI TOF mass spectrometry was carried out by Advanced Chemical Equipment and Instrumentation Facility at the Faculty of Chemistry, Adam Mickiewicz University in Poznan. Analytical HPLC was performed on Agilent 1200 Series instrument coupled with DAD detector.

2.2. Chemical synthesis and characterization

1,4,8,11,15,18,22,25-Octakis[(2-propoxy)phthalocyanine] zinc(II) (**Pc-1**)

Phthalonitrile derivative **1** was obtained according to the literature procedure [27].
Phthalonitrile **1** (1.952 g, 8 mmol), zinc acetate (826 mg, 4.5 mmol), DBU (1.34 mL, 9 mmol) were stirred in *n*-pentanol (5 mL) at 140 °C for 20 h. After that time, the solvent was evaporated and dry residue was chromatographed. Phthalocyanine **Pc-1** was isolated using silica gel (dichloromethane : methanol; 100:1) and repurified using reverse phase column chromatography (methanol : dichloromethane; 7:2) to give a solid green (260 mg, 12.5% yield). TLC R_f = 0.47 (dichloromethane : methanol, 10:1); UV–Vis, λ(ε); DMF: 325 nm (4.13), 408 (4.00), 746 nm (4.64); DMSO: 325 (4.05), 405 (3.88), 750 nm (4.52); MS (MALDI) m/z 1040 $[M+H]^+$; ^{1}H NMR (400 MHz, Pyr) δ (ppm) 7.77 (s, 8H, ArH), 5.33 (m, 8H, OC<u>H</u>), 1.73 (d, 48H, ^3J= 6.0 Hz, OCH(C<u>H</u>$_3$)$_2$; ^{13}C NMR (100 MHz, Pyr) δ (ppm) 153.34, 151.74, 130.53, 123.15, 75.78, 23.54; Chemical purity assessed by HPLC method: 97.35–99.04% (Supplementary data). Crystal Data for **Pc-1**: $C_{61}H_{69}N_9O_8Zn$ (M =1121.62 g/mol): monoclinic, space group $P2_1/c$, a = 11.2922(2) Å, b = 17.0375(3) Å, c = 29.5576(5) Å, β = 98.909(2)°, V = 5618.01(17) Å [28], Z = 4, T = 100.15 K, μ(MoKα) = 0.501 mm-1, D_{calc} = 1.326 g/cm^3, 38236 reflections measured (5.642° ≤ 2Θ ≤ 51.364°), 10616 unique (R_{int} = 0.0349, R_{sigma} = 0.0488) which were used in all calculations. The final R_1 was 0.0365 (I > 2σ(I)) and wR_2 was 0.0847 (all data).

2.3. X-ray studies

Green single crystals of **Pc-1 (**CCDC 1815755) were grown by slow evaporation of pyridine solution at room temperature. The diffraction intensities were collected at 100 K with an Oxford Diffraction Xcalibur diffractometer using fine focus Mo Enhance X-ray source. The data were processed using the CrysAlisPro software [29]. The structure was solved by direct methods and refined by the full-matrix least-squares on F^2 using SIR2014 [30] and SHELXL-2016 [28] programs, respectively. Non-hydrogen atoms were refined anisotropically. All H-atoms were placed at idealized positions and included in the refinement as riding on their pivot atoms with U_{iso}(H) = 1.2$_{eq}$(C) or 1.5$_{eq}$ (CH_3). Summary of the **Pc-1** structure determination is given in Tab. S1. The asymmetric unit with atom labeling scheme is shown in Fig. S1.

2.4. Optical study

2.4.1. Singlet oxygen generation measurements

Singlet oxygen generation assay was performed according to the procedure described in details previously [31–33]. Irradiation was performed at a wavelength corresponding to the Q-band maximum of studied **Pc-1**. Experiments were carried out at ambient temperature under air conditions in DMF and DMSO solutions.

2.4.2. Photostability determination

Evaluation of photodegradation processes was performed following the method described before [31,32,34]. Experiments were carried out at ambient temperature under air conditions in DMF and DMSO.

2.4.3. Emission study

Steady-state fluorescence study was performed according to the method described before [33-35]. Experiments were carried out at ambient temperature under air conditions in DMF and DMSO. Time-resolved fluorescence studies were carried out in anhydrous DMF at the same conditions using a home-built experimental setup based on a femtosecond laser source (Spectra Physics MaiTai) tunable in the range of 690–1020 nm and a Time-Correlated Single Photon Counting (TCSPC) module HydraHarp400 from PicoQuant. Details of the experimental setup are presented in the Supplementary data.

2.4.4. Lipid vesicles preparation

Lipid vesicles were prepared according to the method described by Dragicevic-Curic and co-workers [35]. These systems consist of phospholipids supplied by Avanti Polar Lipids Inc. (Alabaster, AL, USA): POPC (1-palmitoyl-2-oleoyl-sn-glycero-3-phosphocholine) and DOTAP (N-[1-(2,3-dioleoyloxy)propyl]-N,N,N-trimethylammonium chloride, 25 mg/mL). POPC and DOTAP dissolved in chloroform were mixed in molar ratio 8:2. Next, chloroform solution of **Pc-1** was added to lipids mixture in chloroform. The obtained mixture was taken under reduced pressure at 30 °C and chloroform was evaporated. In the next step, 3.3% w/v of ethanol was added to the dried residue and the mixture was vortexed for 5 min. Then, sterile phosphate-buffered saline (PBS) was added to the mixture and subjected to additional 5 min of vortexing. The final stage was the extrusion of formed lipid vesicles through polycarbonate membranes of 200 nm pore size with syringe extruder (Avanti Polar Lipids) (21 times). Formed unified vesicles were stored in a refrigerator at 2–8 °C and protected from light. Vesicles size and their distribution were measured with Zetasizer Nano ZS (Malvern).

2.4.5. In vitro photodynamic activity against bacteria

2.4.5.1. Bacterial cultures

Enterococcus faecalis and *Escherichia coli* strains were purchased from American Type Culture Collection (ATCC; *E. faecalis* ATCC 29212; *E. coli* ATCC 25922). Tested strains were cultured aerobically in BHI broth at 36°C ± 1°C for 18–20 h. Then, microorganisms were harvested by centrifugation (3000 rpm for 15 min), re-suspended in 10 mM phosphate buffered saline (PBS, pH = 7.0) and diluted in PBS to a final concentration of *ca.* 10^7 colony forming units (CFU)/mL.

2.4.5.2. Dark activity

Aliquots of a standardized microbial suspension were placed in the wells of a microtitration plate, then solutions containing different concentrations of the studied compound incorporated in the lipid vesicles formulation were added to each well except controls and bacteria, and incubated for 20 min. Bacterial suspension from each well, after dilution, was grown on tryptic soy agar (TSA) plates. After the incubation period (20 h at 36°C ± 1°C), the viability of bacteria was calculated by counting the number of colony forming units (CFUs). The log reduction of living bacteria in each sample was determined. Experiments were performed in triplicates.

2.4.5.3. Light-dependent activity

Light activity evaluation was performed similarly to the dark one, with irradiation of the culture after incubation time of 20 min. Bacteria were irradiated at room temperature with high power LED MultiChip Emitters (60 high-efficiency AlGaAs diode chips, Roithner LaserTechnik GmbH, Vienna, Austria) with maximum wavelength 735 nm at a fixed total light dose 30 J/cm^2.

2.5. Microtox® analysis

Experiments have been performed according to 81.9% Microtox® test protocol with Microtox Model 500 analyzer and MicrotoxOmni software (Modern Water, Inc.) [36,37].

3. Results and discussion

Phthalocyanine derivative **Pc-1** (Fig. 1) was synthesized according to a two-step procedure. Firstly, 3,6-dihydroxyphthalonitrile was treated with 2-bromopropane in the presence of potassium carbonate as a base to give phthalonitrile derivative **1** following the literature method [27]. Compound **1** was subjected to the macrocyclization reaction with zinc acetate and 1,8-diazabicyclo(5.4.0)undec-7-ene as a base in *n*-pentanol to give phthalocyanine

derivative **Pc-1** (13% yield). The identity of the obtained compound was confirmed using UV-Vis spectrophotometry, MS MALDI spectrometry, and NMR spectroscopy.

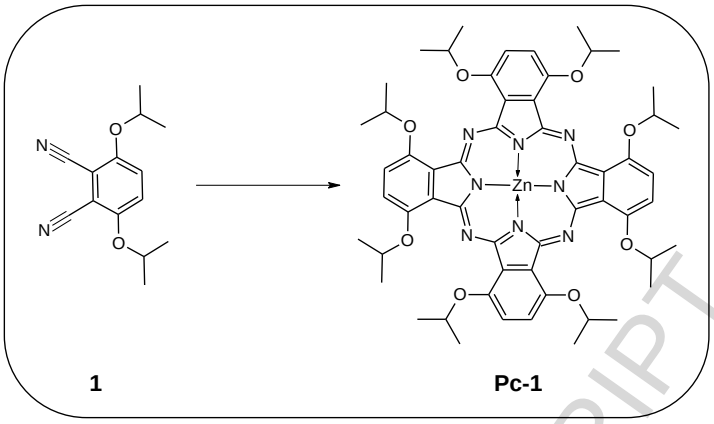

Fig. 1. Synthesis of **Pc-1**: (i) $Zn(OAc)_2$, DBU, *n*-pentanol, reflux

X-ray structural analysis revealed that zinc(II) phthalocyanine **Pc-1** crystallizes in the space group $P2_1/c$ with one molecule per asymmetric unit. The central Zn(II) cation is situated 0.3800(8) Å from the N4-plane formed by four aza-nitrogens and exhibits distorted square-pyramidal coordination geometry being coordinated by the isoindole nitrogen atoms and the N atom of the apical pyridine ligand. Zn—N distances range from 2.017(1) to 2.031(2) Å (Tab. S2). Phthalocyanine **Pc-1** is highly overcrowded due to eight non-peripheral 2-propoxy substituents at the isoindole groups resulting in a strong non-planarity of the π-system of the **Pc-1** core (Fig. 2). Diverse orientations of 2-propoxy groups relative to the heterocycle reduce the highest possible C_4 symmetry of the molecule to C_1. A steric hindrance between the neighboring 2-propoxy groups is released mainly by the twist along the C-N bonds connecting the isoindole units and the distortion of planar isoindole system (combination of a propeller-like distortion and a bending of the fused rings). The **Pc-1** core adopts a saddle-like shape with the isoindole units A/C and the units B/D tilted in the opposite directions of the aza-N4-plane. The dihedral angles between the planes of the pyrrole rings A and C, and B and D, are 21.4(1)° and 11.9(1)°, respectively. Analysis of **Pc-1** supramolecular architecture reveals that in the absence of functional groups able to form strong intermolecular interactions only weak forces stabilize the 3D crystal structure. Zig-zag chains are formed by π-π stacking interactions between virtually coplanar six-membered isoindole A and the axial pyridine rings of the two fold screw axis related molecules. The distance between ring centroids is 3.52 Å. Parallel chains are arranged into layers perpendicular to the cell c axis (Fig. S2). Weak intra- and interlayer C-H…O interactions between 2-propoxy substituents stabilize the 3D crystal network.

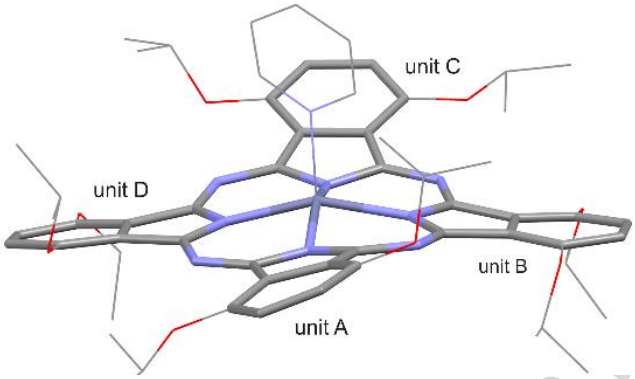

Fig. 2 Out-of-plane distortion of **Pc-1** core. 2-Propoxy substituents are drawn in wireframe style. Hydrogen atoms are omitted for clarity

UV-Vis absorption spectra of the studied phthalocyanine in various solvents reveal two characteristic bands, first in the blue region and the second in the red one (Fig. 3c). Shape and bands intensities are typical for phthalocyanine derivatives previously described [31,38,39].

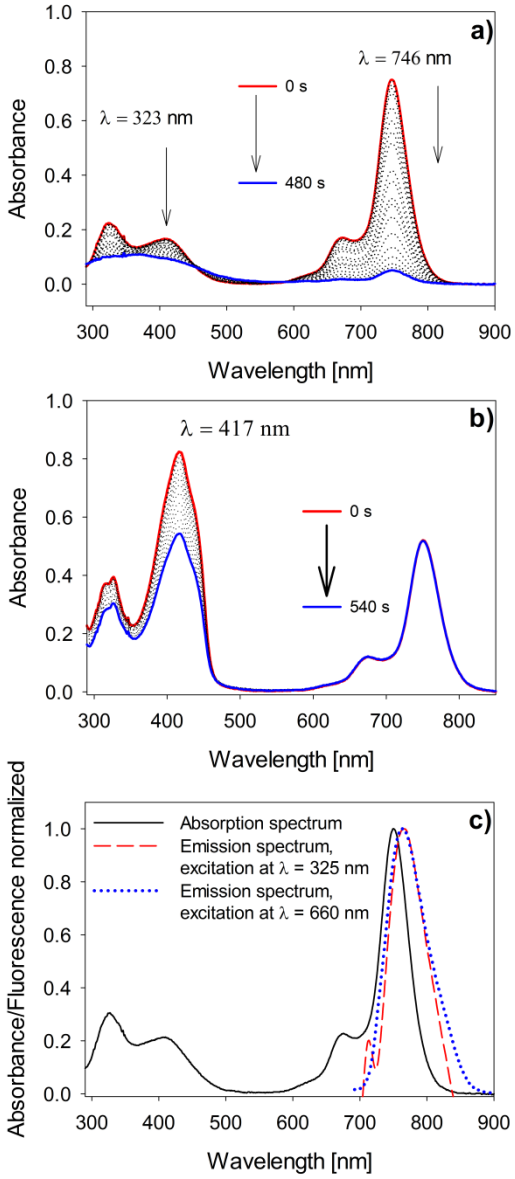

Fig. 3. UV-Vis absorption and emission spectra recorded for **Pc-1**: (a) photostability measurements in DMF; (b) singlet oxygen generation study with DPBF as a chemical quencher in DMSO; (c) fluorescence measurements in DMSO.

Steady-state emission properties of the studied phthalocyanine were investigated in DMF and DMSO. The fluorescence spectrum profile is a mirror image of that one for absorption (Fig. 3c). It suggests that geometry of an excited molecule does not differ from a molecule in the ground state. **Pc-1** shows very low quantum yield of fluorescence, reaching the value of Φ_{FL} = 0.005 and 0.004 in DMF and DMSO, respectively. Low values of fluorescence quantum yield of **Pc-1** are reflected in its sub-nanosecond fluorescence lifetimes, e.g. the fluorescence decay recorded in DMF (Fig. 4a) can be quite well fitted with a

monoexponential function with a decay time of 0.67 ± 0.02 ns. However, the residuals obtained for the mono-exponential fit are apparently structured (Fig. 4b). A biexponential fit results in completely flat residuals (Fig. 4c) and decay times equal to 0.75 ± 0.03 ns (normalized pre-exponential factor 0.62) and 0.44 ± 0.03 ns (normalized pre-exponential factor 0.38).

Nevertheless, the very small difference in the quality of the mono- and biexponential fits suggests that the structure of residuals of the monoexponential fit results not from the presence of two distinct fluorescence decay components of different fluorophores, but rather from a distribution of fluorescence lifetimes of a single chemical species. The distribution can be due to different rotamers with respect to the orientation of 2-propoxy substituents. Presence of aggregates in the sample, which could result in the appearance of the shorter decay component, was excluded by fluorescence lifetime measurements in DMF with various concentrations of pyridine. It is therefore justified to identify the fluorescence lifetime of **Pc-1** in DMF with the decay time obtained from the monoexponential fit. A more precise approach is the calculation of the fluorescence lifetime as a weighted average of two decay times of the biexponential fit function (with the fractional intensities of the decay components as weights), [37], equal to 0.63 ± 0.03 ns (Tab. 2).

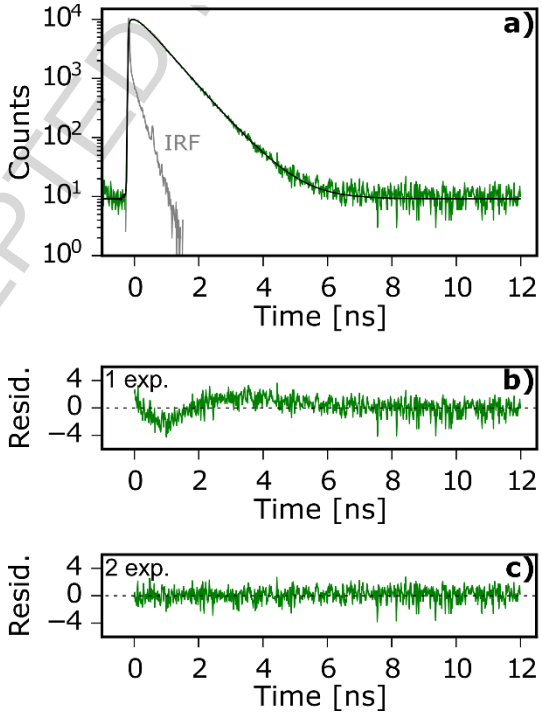

Fig. 4. (a) Fluorescence decay of **Pc-1** in DMF solution recorded with excitation at 740 nm and detection at 760 nm; Residuals of fits of the fluorescence decay of **Pc-1**: (b) monoexponential; (c) biexponential.

Previous studies on the non-peripherally alkoxy-substituted phthalocyanines have revealed that the macrocycle core can be easily protonated [40–46]. The above-mentioned observation applies to **Pc-1** as well. Titration of **Pc-1** in DMF solution with sulfuric acid leads to a gradual conversion of the non-protonated molecule into its monoprotonated form and subsequently into the *trans*-diprotonated form, seen as the origin of new broadened and red-shifted absorption bands (Fig. 5). Two pronounced isosbestic points, at 773 and 845 nm, can be distinguished in the spectral evolution (Supplementary data, Fig. S3 a, b), which indicates that the protonation of the molecule within the acid concentrations in the range of 41 µM – 56 mM is not accompanied by other processes. Further addition of the acid resulted in decomposition of the phthalocyanine. Therefore its tri- and tetraprotonated forms could not be obtained.

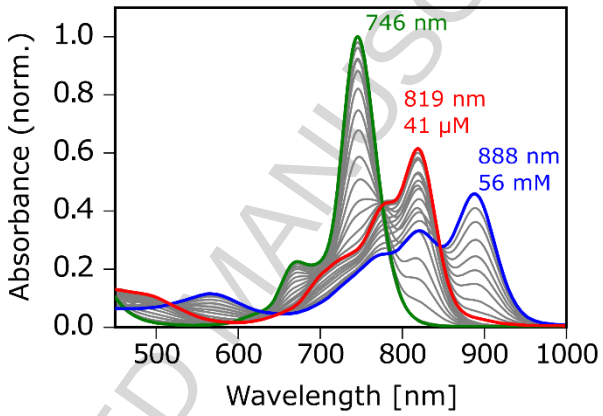

Fig. 5. Absorption spectra of **Pc-1** in DMF solution recorded during titration with sulfuric acid. Spectra that can be attributed to mono- and diprotonated forms recorded at acid concentrations shown are printed with thick red and blue lines, respectively. All spectra are normalized to the maximum of the absorption of the non-protonated form (green).

Analysis of the absorption spectra obtained as a result of the titration according to the Hill formalism [42,47], following the scheme described in detail in reference [43], allows for estimation of the formation constants of the mono- and diprotonated forms, log K_1 = 4.8, log K_2 = 2.8, respectively (corresponding Hill plots are shown in Fig. S3 c, d). Value of log K_1 is significantly larger than obtained earlier for analogues of **Pc-1** with longer alkoxy chains [43] indicating stronger tendency for protonation. This effect can be explained by a more electron-donating character of 2-propoxy groups than that of 1,4,7-trioxanonyl and *n*-butoxy substituents, resulting in higher reactivity of the **Pc-1** macrocycle than of the other molecules. This trend is not maintained for log K_2 which for **Pc-1** is slightly smaller than the value obtained for its *n*-butoxy analogue but is significantly larger for the trioxanonyl analogue.

This could be as a result of a disturbance of the macrocycle by monoprotonation, whose effect prevails over small differences in the electron-donating character of the 2-propoxy and *n*-butoxy substituents. Nevertheless, the effect of the monoprotonation does not override the much larger difference between the electron-donating ability of trioxanonyl and *n*-propoxy substituents.

Protonation of **Pc-1** significantly shortens the fluorescence lifetime due to the increase in the non-radiative deactivation rate, according to the energy gap law [48] in protonated molecules (Fig. 6). Fluorescence decays, measured in different conditions, including acid concentration, excitation/detection wavelengths, in which the monoprotonated form should bring the main contribution, are dominated by the fast component (0.36 ns) with only a small (normalized pre-exponential factor 0.03) contribution of the longer one (0.78 ns). The former decay time should be identified with the fluorescence lifetime of the monoprotonated form, whereas the latter most probably results from the presence of a small population of non-protonated molecules or reflects a small distribution of the fluorescence lifetimes, as in the case of non-protonated molecules. Fluorescence decay recorded for the diprotonated form is clearly monoexponential with a decay time shortened down to 0.14 ns. Summary of the fluorescence lifetimes of the protonated forms of **Pc-1** is shown in Tab. 2 and plots of the residuals are shown in supplementary data – Fig. S4.

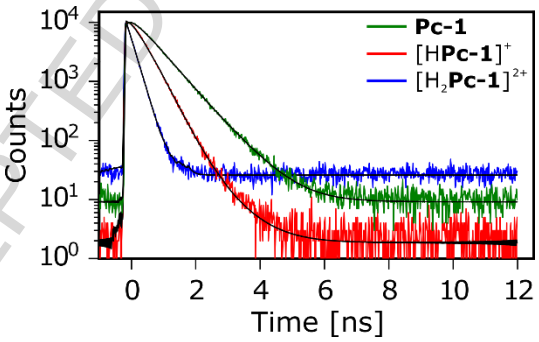

Fig. 6. Fluorescence decays of mono- $[H\mathbf{Pc\text{-}1}]^{+}$ and diprotonated $[H_2\mathbf{Pc\text{-}1}]^{2+}$ forms of **Pc-1,** compared with the fluorescence decay of the parent molecule, recorded at conditions indicated in Tab. 1.

Tab. 1. Fluorescence lifetimes of **Pc-1** and its protonated forms measured in DMF solution at indicated excitation and detection wavelengths

	Acid conc.	**Excitation wavelength (nm)**	**Detection wavelength (nm)**	**Decay times (ns)**	**Reduced χ^2**
Pc-1	0	740	760	**Monoexp.** 0.67±0.02	1.77
				Biexp. 0.75±0.03 (0.62) 0.44±0.03 (0.38)	1.34
				Average 0.63±0.03	
[H**Pc-1**]$^{+}$	41 μM	790	830	0.36±0.01 (0.97) 0.78±0.02 (0.03)	1.43
[H_2**Pc-1**]$^{2+}$	56 mM	890	910	0.14±0.01	1.14

Singlet oxygen generation study showed the moderate potential of **Pc-1** in singlet oxygen production. The changes recorded in the spectra of **Pc-1** and DPBF mixture are presented in Fig. 3b. For the photodynamic therapy, the formation of singlet oxygen is crucial [22]. Quantum yields of singlet oxygen generation calculated for **Pc-1** were equal to 0.18 and 0.16 in DMF and DMSO, respectively (Tab. 2).

Tab. 2. Photodynamic parameters, antibacterial activity and size of lipid vesicles for studied zinc phthalocyanine **Pc-1**

photochemical properties								**reduction in bacterial growth [log]**			**Size of lipid vesicles**	
Φ_Δ	DMF	0.18	Φ_P	DMF	$3.06 \cdot 10^{-4}$	Φ_{FL}	DMF	0.005	*Enterococcus faecalis*	30 J/cm^2 735 nm 100 μM	5.7	Mean diameter ± SD [nm]	PDI index
	DMSO	0.16		DMSO	$1.23 \cdot 10^{-5}$		DMSO	0.004	*Escherichia coli*		0.5	174±4	0.23

Also, the "heavy atom effect" was observed comparing the singlet oxygen quantum yield for **Pc-1** with the results of our group's latest published work on magnesium phthalocyanine containing 2-propoxy substituents at non-peripheral positions. The magnesium derivative showed singlet oxygen quantum yield Φ_Δ = 0.03 and 0.04 in DMSO and DMF, respectively [49]. An introduction eight of 2-propoxy groups to the structure of phthalocyanine (**Pc-1**) results in lowering the quantum yield values in comparison to unsubstituted zinc(II) phthalocyanine (Φ_Δ values equal 0.56 in DMF and 0.67 in DMSO). The above phenomenon can be related to an increasing non-radiative deactivation due to the presence of alkyl and alkoxy substituents in the structure [50].

During irradiation of **Pc-1** dissolved in DMF or DMSO with visible light, the intensity of their absorption spectra decreased (Fig. 3a). Moreover, a formation of an additional band was not noticed. It suggests that photodecomposition phenomenon reveals photobleaching pathway. For **Pc-1**, it was assessed that the quantum yields of photodecomposition (Φ_P) processes equal $3.1 \cdot 10^{-4}$ and $1.2 \cdot 10^{-5}$ in DMF and DMSO, respectively. The photostability of the studied phthalocyanine **Pc1** is comparable with the stability of peripherally substituted phthalocyanines with oxy moieties presented by Chauke and co-workers (**I**, **II**; Fig. 7) [33]. Earlier our group studied trioxanonyl zinc phthalocyanine (**III**; Fig. 7) [22], which in comparison with **Pc-1** revealed 2.7-fold better photostability in DMF. Interestingly, **Pc-1** dissolved in DMSO showed the same photostability level as [1,4,8,11,15,18,22,25-octakis(1,4,7-trioxanonyl)phthalocyanine] zinc(II) (**III**) previously studied in the same solvent [43].

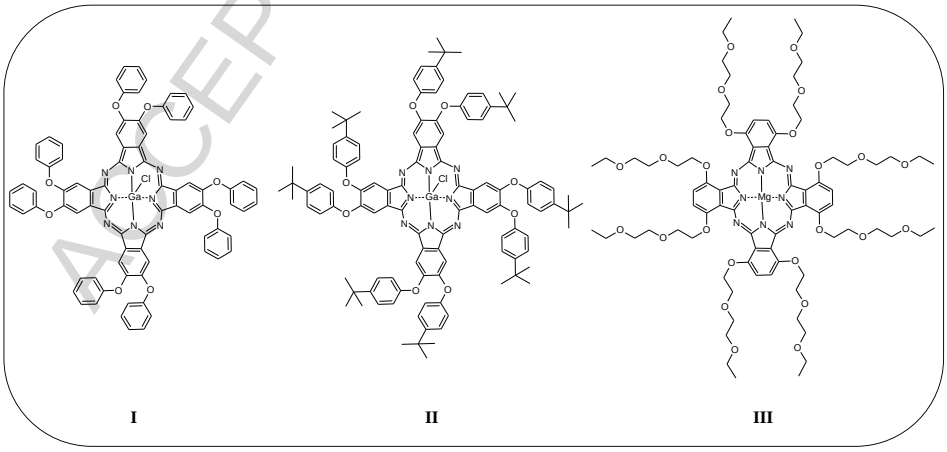

Fig. 7. Chemical structures of phthalocyanines studied by Chauke and co-workers – **I**, **II** [33]; Sobotta and co-workers – **III** [22]

For photodynamic inactivation of bacteria, novel phthalocyanine **Pc-1** was incorporated into lipid vesicles containing ethanol in relatively low concentration. According

to the literature, many types of lipid vesicles embodying ethanol have been considered so far [25]. The amount of ethanol in lipid formulation is known to influence many features of vesicles, including diameter and skin penetration potential. Therefore in many literature studies, ethanol has been used in lipid mixtures in various concentrations [51]. On the one hand, vesicular systems, known as ethosomes, containing ethanol in relatively high concentrations (20-50%) revealed enhanced skin permeation to many active pharmaceutical ingredients. On the other hand, invasomes containing permeability enhancers, such as terpenes and ethanol at lower concentrations (typically from 0% to 3.3%) were also efficient in delivering of pharmaceutically active ingredients [25]. Invasomes in comparison to liposomes are more flexible and enable the delivery of drug molecules more effectively. Some initial studies have been conducted showing the effectiveness of invasomes for PACT [26]. As a model bacteria to *in vitro* photodynamic inactivation tests, *Enterococcus faecalis* as a Gram-positive bacteria and *Escherichia coli* as a Gram-negative were chosen. *E. faecalis* is known as the main problem in dental pulp infections. It is a facultative anaerobe, and therefore it does not suffer from a lack of oxygen [52,53]. Usually in dental practice sodium chlorate(I) (NaClO) is applied as a bactericidal drug [54]. It was reported that the dental tubules can be penetrated by *E. faecalis* up to 300 – 1000 μm, whereas NaClO reaches only inside to 150 μm. Unfortunately, this phenomenon enables the bacteria to survive the treatment procedure [55–57]. It was found that the treatment of dentine tubules with invasomes can be considered as an alternative approach for the conventional endodontic treatment procedure [35,57]. Because of rising bacterial resistance in conventional treatment, the development of novel techniques for bacteria eradication is becoming increasingly important. It should be pointed out that some *Enterococcus faecalis* strains reveal resistance to β-lactams (cephalosporins), clindamycin, macrolides, sulfonamides and may reveal resistance to other antibiotics, e.g. glycopeptides (vancomycin), tetracyclines [58–60]. In our study, researched **Pc-1** in lipid vesicles containing the optimal concentration of ethanol inactivated *E. faecalis* at the concentration of 100 μM, when excited with 735 nm light at light dose 30 J/cm^2. For mentioned dosimetry, the number of viable cells were reduced to the level of 5.7 log.

Escherichia coli was studied as an example of Gram-negative bacteria, which is present in the gastrointestinal tract in humans. Commonly *E. coli* exhibit a positive influence on the human digestive process. Besides, there are known *E. coli* strains with specific virulence, which can cause diseases including enteric/diarrhoeal problems, urinary system infections or even sepsis[61]. As it was expected, studied **Pc-1** revealed no significant

photoinactivation ability against *E. coli*. It can be connected with a lack of positive charges on the periphery of the molecule, which is more important for photodynamic inactivation of Gram-negative than positive bacteria [62].

As an extension of our study, 81.9% screening test with Microtox® system was performed, which allowed us to determine the dark toxicity of the studied compound. Microtox® system is based on bioluminescence measurement of *Vibrio fischeri*, which under exposition to a toxic agent dies and loses its bioluminescence ability [36,37,63]. Studied phthalocyanine **Pc-1** has revealed very low level of dark toxicity with luminescence inhibition at 7.9% after 5 min exposition and 5.3% after 15 min.

4. Conclusions

In this paper, we presented the synthesis of novel zinc(II) phthalocyanine bearing eight 2-propoxy substituents (**Pc-1**). Phthalocyanine macrocycle **Pc-1** (Fig. 1) was synthesized according to a two-step procedure, starting from 3,6-di(2-propoxy)phthalonitrile. The obtained phthalocyanine was characterized by UV-Vis spectrophotometry, spectrofluorimetry, MS MALDI spectrometry and NMR spectroscopy. As shown by X-ray crystallography, a steric hindrance between eight non-peripheral 2-propoxy substituents leads to distortion of the planar π-electron system of the macrocycle core. The UV-Vis absorption spectra in various solvents of the studied phthalocyanine reveal two characteristic bands, first in the blue region and second in the red one. The bands shapes and intensities in the UV-Vis are typical of phthalocyanine derivatives. Low values of fluorescence quantum yield of **Pc-1** are reflected in its sub-nanosecond fluorescence lifetimes.

Titration of the studied phthalocyanine with sulfuric acid in DMF solution led to a gradual conversion of the non-protonated molecule into its monoprotonated form and subsequently into the *trans*-diprotonated form. Further addition of the acid resulted in decomposition of the phthalocyanine. Therefore its tri- and tetraprotonated forms could not be obtained. Moreover, the usability of PACT against bacteria was assessed. The presented phthalocyanine studied, has revealed moderate singlet oxygen generation ability equal to 0.18 and 0.16 in DMF and DMSO, respectively. Moderate photostability has been noticed with quantum yield of photodecomposition equal $3.1 \cdot 10^{-4}$ and $1.2 \cdot 10^{-5}$ in DMF and DMSO, respectively. Also, the phthalocyanine studied revealed the low potential for fluorescence emission with yields 0.005 and 0.004 in DMF and DMSO, respectively. *In vitro* PACT biological study indicates moderate inactivation of *Enterococcus faecalis* equal to 5.7 log

reduction in bacterial growth and no activity against *Escherichia coli* at 100 μM for lipid vesicles embodying zinc(II) phthalocyanine bearing eight 2-propoxy substituents.

Acknowledgments

This work was supported by the National Science Centre, Poland under Grant No. 2016/21/B/NZ9/00783.

Appendix A. Supplementary data

Supplementary data to this article can be found online at

The crystallographic data in CIF format have been deposited at the Cambridge Crystallographic Data Centre, CCDC 1815755. They can be obtained free of charge via https://www.ccdc.cam.ac.uk/structures/

References

[1] A. de la Escosura, O. Trukhina, T. Torres, Dual Role of Phthalocyanines in Carbon Nanostructure-Based Organic Photovoltaics, in: Springer Berlin Heidelberg, Berlin, Heidelberg, 2013. http://link.springer.com/10.1007/430_2013_113 (accessed October 12, 2016).

[2] M.-E. Ragoussi, T. Torres, New generation solar cells: concepts, trends and perspectives, Chem Commun. 51 (2015) 3957–3972. doi:10.1039/C4CC09888A.

[3] M.-E. Ragoussi, T. Torres, Organic Photovoltaics, Rev. Virtual Quím. 7 (2015). doi:10.5935/1984-6835.20150007.

[4] R.R. Allison, G.H. Downie, R. Cuenca, X.-H. Hu, C.J. Childs, C.H. Sibata, Photosensitizers in clinical PDT, Photodiagnosis Photodyn. Ther. 1 (2004) 27–42. doi:10.1016/S1572-1000(04)00007-9.

[5] J.F. Lovell, T.W.B. Liu, J. Chen, G. Zheng, Activatable Photosensitizers for Imaging and Therapy, Chem. Rev. 110 (2010) 2839–2857. doi:10.1021/cr900236h.

[6] D. Wöhrle, G. Schnurpfeil, S.G. Makarov, A. Kazarin, O.N. Suvorova, Practical Applications of Phthalocyanines – from Dyes and Pigments to Materials for Optical, Electronic and Photo-electronic Devices, Macroheterocycles. 5 (2012) 191–202. doi:10.6060/mhc2012.120990w.

[7] P. Skupin-Mrugalska, L. Sobotta, M. Kucinska, M. Murias, J. Mielcarek, N. Duzgunes, Cellular Changes, Molecular Pathways and the Immune System Following Photodynamic Treatment, Curr. Med. Chem. 21 (2014) 4059–4073.

[8] K. Ishii, Functional singlet oxygen generators based on phthalocyanines, Coord. Chem. Rev. 256 (2012) 1556–1568. doi:10.1016/j.ccr.2012.03.022.

[9] M.C. DeRosa, R.J. Crutchley, Photosensitized singlet oxygen and its applications, Coord. Chem. Rev. 233 (2002) 351–371.

[10] L. Sobotta, P. Skupin – Mrugalska, J. Mielcarek, T. Goslinski, J. Balzarini, Photosensitizers Mediated Photodynamic Inactivation Against Virus Particles, Mini-Rev. Med. Chem. 15 (2015) 1–1. doi:10.2174/1389557515666150415151505.

[11] M.R. Hamblin, Antimicrobial photodynamic inactivation: a bright new technique to kill resistant microbes, Curr. Opin. Microbiol. 33 (2016) 67–73. doi:10.1016/j.mib.2016.06.008.

[12] R.R. Allison, C.H. Sibata, Oncologic photodynamic therapy photosensitizers: A clinical review, Photodiagnosis Photodyn. Ther. 7 (2010) 61–75. doi:10.1016/j.pdpdt.2010.02.001.

[13] N.A. Kuznetsova, O.L. Kaliya, Heterogenized metallophthalocyanines for photodynamic microorganism inactivation: an overview of our experience, Macroheterocycles. 8 (2015) 8–19. doi:10.6060/mhc141243k.

[14] Z. Chen, S. Zhou, J. Chen, L. Li, P. Hu, S. Chen, M. Huang, An effective zinc phthalocyanine derivative for photodynamic antimicrobial chemotherapy, J. Lumin. 152 (2014) 103–107. doi:10.1016/j.jlumin.2013.10.067.

[15] M. Wainwright, T. Maisch, S. Nonell, K. Plaetzer, A. Almeida, G.P. Tegos, M.R. Hamblin, Photoantimicrobials—are we afraid of the light?, Lancet Infect. Dis. 17 (2017) e49–e55. doi:10.1016/S1473-3099(16)30268-7.

[16] Z. Chen, Y. Zhang, D. Wang, L. Li, S. Zhou, J.H. Huang, J. Chen, P. Hu, M. Huang, Photodynamic antimicrobial chemotherapy using zinc phthalocyanine derivatives in treatment of bacterial skin infection, J. Biomed. Opt. 21 (2016) 018001–018001.

[17] M.S. Baptista, M. Wainwright, Photodynamic antimicrobial chemotherapy (PACT) for the treatment of malaria, leishmaniasis and trypanosomiasis, Braz. J. Med. Biol. Res. 44 (2011) 1–10. doi:10.1590/S0100-879X2010007500141.

[18] C.M. Cassidy, R.F. Donnelly, J.S. Elborn, N.D. Magee, M.M. Tunney, Photodynamic Antimicrobial Chemotherapy (PACT) in combination with antibiotics for treatment of Burkholderia cepacia complex infection, J. Photochem. Photobiol. B. 106 (2012) 95–100. doi:10.1016/j.jphotobiol.2011.10.010.

[19] M. Kryjewski, T. Goslinski, J. Mielcarek, Functionality stored in the structures of cyclodextrin–porphyrinoid systems, Coord. Chem. Rev. 300 (2015) 101–120. doi:10.1016/j.ccr.2015.04.009.

[20] P. Skupin-Mrugalska, J. Piskorz, T. Gośliński, J. Mielcarek, K. Konopka, N. Düzgüneş, Current status of liposomal porphyrinoid photosensitizers, Drug Discov. Today. 18 (n.d.) 776–784. doi:10.1016/j.drudis.2013.04.003.

[21] D.T. Mlynarczyk, S. Lijewski, M. Falkowski, J. Piskorz, W. Szczolko, L. Sobotta, M. Stolarska, L. Popenda, S. Jurga, K. Konopka, N. Düzgüneş, J. Mielcarek, T. Goslinski, Dendrimeric Sulfanyl Porphyrazines: Synthesis, Physico-Chemical Characterization, and Biological Activity for Potential Applications in Photodynamic Therapy, ChemPlusChem. 81 (2016) 460–470. doi:10.1002/cplu.201600051.

[22] L. Sobotta, M. Wierzchowski, M. Mierzwicki, Z. Gdaniec, J. Mielcarek, L. Persoons, T. Goslinski, J. Balzarini, Photochemical studies and nanomolar photodynamic activities of phthalocyanines functionalized with 1,4,7-trioxanonyl moieties at their non-peripheral positions, J. Inorg. Biochem. 155 (2016) 76–81. doi:10.1016/j.jinorgbio.2015.11.006.

[23] M. Kucinska, P. Skupin-Mrugalska, W. Szczolko, L. Sobotta, M. Sciepura, E. Tykarska, M. Wierzchowski, A. Teubert, A. Fedoruk-Wyszomirska, E. Wyszko, M. Gdaniec, M. Kaczmarek, T. Goslinski, J. Mielcarek, M. Murias, Phthalocyanine Derivatives Possessing 2-(Morpholin-4-yl)ethoxy Groups As Potential Agents for Photodynamic Therapy, J. Med. Chem. 58 (2015) 2240–2255. doi:10.1021/acs.jmedchem.5b00052.

[24] J. Dlugaszewska, W. Szczolko, T. Koczorowski, P. Skupin-Mrugalska, A. Teubert, K. Konopka, M. Kucinska, M. Murias, N. Düzgüneş, J. Mielcarek, T. Goslinski, Antimicrobial and anticancer photodynamic activity of a phthalocyanine photosensitizer with N -methyl morpholiniumethoxy substituents in non-peripheral positions, J. Inorg. Biochem. 172 (2017) 67–79. doi:10.1016/j.jinorgbio.2017.04.009.

[25] D.. Verma, A. Fahr, Synergistic penetration enhancement effect of ethanol and phospholipids on the topical delivery of cyclosporin A, J. Controlled Release. 97 (2004) 55–66. doi:10.1016/j.jconrel.2004.02.028.

[26] A. Ossmann, S. Kranz, G. Andre, A. Völpel, V. Albrecht, A. Fahr, B.W. Sigusch, Photodynamic killing of Enterococcus faecalis in dentinal tubules using mTHPC incorporated in liposomes and invasomes, Clin. Oral Investig. 19 (2015) 373–384. doi:10.1007/s00784-014-1271-9.

[27] T.P. Forsyth, D.B.G. Williams, A.G. Montalban, C.L. Stern, A.G.M. Barrett, B.M. Hoffman, A Facile and Regioselective Synthesis of Trans-Heterofunctionalized Porphyrazine Derivatives, J. Org. Chem. 63 (1998) 331–336. doi:10.1021/jo971683c.

[28] G.M. Sheldrick, Crystal structure refinement with *SHELXL*, Acta Crystallogr. Sect. C Struct. Chem. 71 (2015) 3–8. doi:10.1107/S2053229614024218.

[29] Rigaku Oxford Diffraction (2015). CrysAlisPRO, Rigaku Corporation, Oxford, UK, n.d.

[30] M.C. Burla, R. Caliandro, B. Carrozzini, G.L. Cascarano, C. Cuocci, C. Giacovazzo, M. Mallamo, A. Mazzone, G. Polidori, Crystal structure determination and refinement *via SIR2014*, J. Appl. Crystallogr. 48 (2015) 306–309. doi:10.1107/S1600576715001132.

[31] L. Sobotta, P. Fita, W. Szczolko, M. Wrotynski, M. Wierzchowski, T. Goslinski, J. Mielcarek, Functional singlet oxygen generators based on porphyrazines with peripheral 2,5-dimethylpyrrol-1-yl and dimethylamino groups, J. Photochem. Photobiol. A. 269 (2013) 9–16. doi:10.1016/j.jphotochem.2013.06.018.

[32] I. Seotsanyana-Mokhosi, N. Kuznetsova, T. Nyokong, Photochemical studies of tetra-2, 3-pyridinoporphyrazines, J. Photochem. Photobiol. A. 140 (2001) 215–222.

[33] V. Chauke, A. Ogunsipe, M. Durmuş, T. Nyokong, Novel gallium(III) phthalocyanine derivatives – Synthesis, photophysics and photochemistry, Polyhedron. 26 (2007) 2663–2671. doi:10.1016/j.poly.2007.01.016.

[34] N.A. Kuznetsova, D.A. Makarov, O.A. Yuzhakova, L.I. Solovieva, O. L. Kaliya, Study on the photostability of water-soluble Zn(II) and Al(III) phthalocyanines in aqueous solution, J. Porphyr. Phthalocyanines. 14 (2010) 968–974. doi:10.1142/S1088424610002835.

[35] N. Dragicevic-Curic, D. Scheglmann, V. Albrecht, A. Fahr, Development of different temoporfin-loaded invasomes—novel nanocarriers of temoporfin: Characterization, stability and in vitro skin penetration studies, Colloids Surf. B Biointerfaces. 70 (2009) 198–206. doi:10.1016/j.colsurfb.2008.12.030.

[36] T.X.H. Le, T.V. Nguyen, Z. Amadou Yacouba, L. Zoungrana, F. Avril, D.L. Nguyen, E. Petit, J. Mendret, V. Bonniol, M. Bechelany, S. Lacour, G. Lesage, M. Cretin, Correlation between degradation pathway and toxicity of acetaminophen and its by-products by using the electro-Fenton process in aqueous media, Chemosphere. 172 (2017) 1–9. doi:10.1016/j.chemosphere.2016.12.060.

[37] R. Weltens, K. Deprez, L. Michiels, Validation of Microtox as a first screening tool for waste classification, Waste Manag. 34 (2014) 2427–2433. doi:10.1016/j.wasman.2014.08.001.

[38] E. Fazio, J. Jaramillo-García, G. de la Torre, T. Torres, Efficient Synthesis of ABAB Functionalized Phthalocyanines, Org. Lett. 16 (2014) 4706–4709. doi:10.1021/ol502042r.

[39] N. Nombona, E. Antunes, T. Nyokong, The synthesis and fluorescence behaviour of phthalocyanines unsymmetrically substituted with naphthol and carboxy groups, Dyes Pigments. 86 (2010) 68–73. doi:10.1016/j.dyepig.2009.11.010.

[40] K. Kasuga, K. Yashiki, T. Sugimori, M. Handa, Bathochromic shift of the Q-bands of octakis(p-t-butylbenzyloxy)phthalocyanines with magnesium(II), nickel(II) and copper(II) in a solvent mixture of chloroform and acetic acid, J. Porphyr. Phthalocyanines. 09 (2005) 646–650. doi:10.1142/S1088424605000757.

[41] S. Fukuzumi, T. Honda, T. Kojima, Structures and photoinduced electron transfer of protonated complexes of porphyrins and metallophthalocyanines, Coord. Chem. Rev. 256 (2012) 2488–2502. doi:10.1016/j.ccr.2012.01.011.

[42] T. Honda, T. Kojima, S. Fukuzumi, Control of electron-transfer reduction by protonation of zinc octabutoxyphthalocyanine assisted by intramolecular hydrogen bonding., Chem. Commun. 47 (2011) 7986–7988. doi:10.1039/c1cc12710a.

[43] P. Kasprzycki, L. Sobotta, S. Lijewski, M. Wierzchowski, T. Goslinski, J. Mielcarek, C. Radzewicz, P. Fita, Unusual cis-diprotonated forms and fluorescent aggregates of non-peripherally alkoxy-substituted metallophthalocyanines, Phys Chem Chem Phys. 19 (2017) 21390–21400. doi:10.1039/C7CP04321J.

[44] M.P. Donzello, C. Ercolani, A.A. Gaberkorn, E.V. Kudrik, M. Meneghetti, G. Marcolongo, C. Rizzoli, P.A. Stuzhin, Synthesis, X-ray Crystal Structure, UV/Visible Linear and Nonlinear (Optical Limiting) Spectral Properties of Symmetrical and Unsymmetrical Porphyrazines with Annulated 1,2,5-Thiadiazole and 1,4-Diamyloxybenzene Moieties, Chem. - Eur. J. 9 (2003) 4009–4024. doi:10.1002/chem.200304929.

[45] D.A. Makarov, V.M. Derkacheva, N.A. Kuznetsova, O.L. Kaliya, E.A. Lukyanets, Octa-3,6-hexoxyphthalocyanines: Effect of Protonation on Spectral and Photochemical Properties, Macroheterocycles. 6 (2013) 371–378. doi:10.6060/mhc130951k.

[46] E.A. Safonova, A.G. Martynov, S.E. Nefedov, G.A. Kirakosyan, Y.G. Gorbunova, A.Y. Tsivadze, A Molecular Chameleon: Reversible pH- and Cation-Induced Control of the Optical Properties of Phthalocyanine-Based Complexes in the Visible and Near-Infrared Spectral Ranges, Inorg. Chem. 55 (2016) 2450–2459. doi:10.1021/acs.inorgchem.5b02831.

[47] H. Bisswanger, Enzyme Kinetics. Principles and Methods, WILEY-VCH Verlag GmbH, Weinheim, 2002.

[48] R. Englman, J. Jortner, The energy gap law for radiationless transitions in large molecules, Mol. Phys. 18 (1970) 145–164.

[49] A. Tillo, M. Stolarska, M. Kryjewski, L. Popenda, L. Sobotta, S. Jurga, J. Mielcarek, T. Goslinski, Phthalocyanines with bulky substituents at non-peripheral positions – Synthesis and physico-chemical properties, Dyes Pigments. 127 (2016) 110–115. doi:10.1016/j.dyepig.2015.12.017.

[50] D. Wróbel, A. Boguta, Study of the influence of substituents on spectroscopic and photoelectric properties of zinc phthalocyanines, J. Photochem. Photobiol. A. 150 (2002) 67–76.

[51] E. Touitou, N. Dayan, L. Bergelson, B. Godin, M. Eliaz, Ethosomes — novel vesicular carriers for enhanced delivery: characterization and skin penetration properties, J. Controlled Release. 65 (2000) 403–418. doi:10.1016/S0168-3659(99)00222-9.

[52] Z. Lim, J. Cheng, T. Lim, E. Teo, J. Wong, S. George, A. Kishen, Light activated disinfection: an alternative endodontic disinfection strategy, Aust. Dent. J. 54 (2009) 108–114. doi:10.1111/j.1834-7819.2009.01102.x.

[53] I.B. Jurič, V. Plečko, D.G. Pandurić, I. Anić, The antimicrobial effectiveness of photodynamic therapy used as an addition to the conventional endodontic re-treatment: A clinical study, Photodiagnosis Photodyn. Ther. 11 (2014) 549–555. doi:10.1016/j.pdpdt.2014.10.004.

[54] J.F. Siqueira, A.G. Machado, R.M. Silveira, H.P. Lopes, M. de Uzeda, Evaluation of the effectiveness of sodium hypochlorite used with three irrigation methods in the elimination of Enterococcus faecalis from the root canal, in vitro, Int. Endod. J. 30 (1997) 279–282.

[55] E. Berutti, R. Marini, A. Angeretti, Penetration ability of different irrigants into dentinal tubules, J. Endod. 23 (1997) 725–727. doi:10.1016/S0099-2399(97)80342-1.

[56] L.B. Peters, P.R. Wesselink, J.F. Buijs, A.J. Van Winkelhoff, Viable bacteria in root dentinal tubules of teeth with apical periodontitis, J. Endod. 27 (2001) 76–81.

[57] S.S. Bumb, Assessment of Photodynamic Therapy (PDT) in Disinfection of Deeper Dentinal Tubules in a Root Canal System: An In Vitro Study, J. Clin. Diagn. Res. (2014). doi:10.7860/JCDR/2014/11047.5155.

[58] I. Portenier, T.M. Waltimo, M. Haapasalo, Enterococcus faecalis–the root canal survivor and 'star'in post-treatment disease, Endod. Top. 6 (2003) 135–159.

[59] B. Athanassiadis, P. Abbott, L. Walsh, The use of calcium hydroxide, antibiotics and biocides as antimicrobial medicaments in endodontics, Aust. Dent. J. 52 (2007) S64–S82. doi:10.1111/j.1834-7819.2007.tb00527.x.

[60] K. Fisher, C. Phillips, The ecology, epidemiology and virulence of Enterococcus, Microbiology. 155 (2009) 1749–1757. doi:10.1099/mic.0.026385-0.

[61] J.B. Kaper, J.P. Nataro, H.L.T. Mobley, Pathogenic Escherichia coli, Nat. Rev. Microbiol. 2 (2004) 123–140. doi:10.1038/nrmicro818.

[62] T.N. Demidova, M.R. Hamblin, Effect of Cell-Photosensitizer Binding and Cell Density on Microbial Photoinactivation, Antimicrob. Agents Chemother. 49 (2005) 2329–2335. doi:10.1128/AAC.49.6.2329-2335.2005.

[63] V.R. Urbano, M.G. Maniero, M. Pérez-Moya, J.R. Guimarães, Influence of pH and ozone dose on sulfaquinoxaline ozonation, J. Environ. Manage. 195 (2017) 224–231. doi:10.1016/j.jenvman.2016.08.019.

Graphical abstract

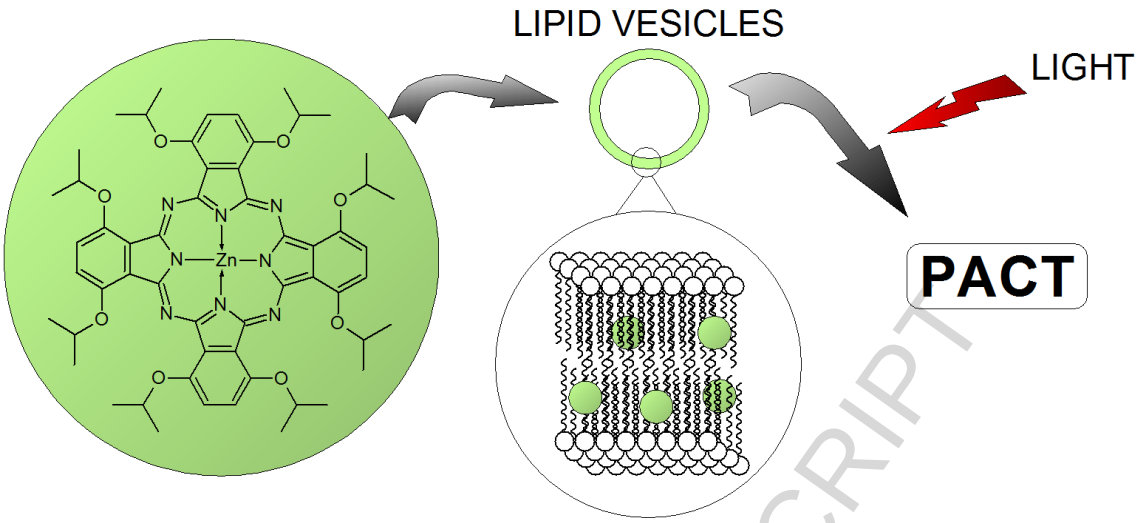

Zinc(II) phthalocyanine with eight non-peripheral 2-propoxy substituents was synthetized. X-ray analysis indicated that overcrowding of the compound leads to a strong out-of-plane distortion of the π-system of the macrocycle core. Although compound excited with red light formed singlet oxygen with a moderate yield, it reduced *Enterococcus faecalis* growth by 5.7 log.

Highlights

- Zinc(II) phthalocyanine bearing eight non-peripheral 2-propoxy substituents was synthetized
- The presented zinc(II) phthalocyanine showed ability for singlet oxygen generation
- X-ray analysis revealed that overcrowding of phthalocyanine leads to strong out-of-plane distortion of macrocycle π-system
- *In vitro* bacteria photoinactivation study revealed the high potential of researched macrocycle against *Enterococcus faecalis*